Electrical control of polariton coupling in intersubband microcavities

Aji A. Anappara, Alessandro Tredicucci, Giorgio Biasiol, and Lucia Sorba

Citation: Applied Physics Letters **87**, 051105 (2005); doi: 10.1063/1.2006976
View online: http://dx.doi.org/10.1063/1.2006976
View Table of Contents: http://scitation.aip.org/content/aip/journal/apl/87/5?ver=pdfcov
Published by the AIP Publishing

Electrical control of polariton coupling in intersubband microcavities

Aji A. Anappara and Alessandro Tredicucci[a)]
NEST-INFM and Scuola Normale Superiore, Piazza dei Cavalieri 7, I-56126 Pisa, Italy

Giorgio Biasiol
NEST-INFM and Laboratorio Nazionale TASC-INFM, AREA Science Park, S 14 Km 163.5, Basovizza, I-34012 Trieste, Italy

Lucia Sorba
NEST-INFM and Laboratorio Nazionale TASC-INFM, AREA Science Park, SS 14 Km 163.5, Basovizza, I-34012 Trieste, Italy and Universitá di Modena e Reggio Emilia, Via Campi 213/A, I-41100 Modena, Italy

(Received 25 March 2005; accepted 16 June 2005; published online 28 July 2005)

We demonstrate the external control of the coupling between the intersubband transition and the photonic mode of a GaAs/AlGaAs microcavity with multiple quantum wells embedded. By electrical gating, the charge density in the wells can be lowered, thereby quenching the intersubband polaritons and reverting the system to uncoupled excitations. The angle-dependent reflectance measurements are in good agreement with theoretical calculations performed in the transfer matrix formalism. The experiment shows the prospects offered by intersubband microcavities through manipulation of the system ground state. © *2005 American Institute of Physics*.
[DOI: 10.1063/1.2006976]

Intersubband optical phenomena involve the transition between two-dimensional electronic levels within the conduction band of semiconductor heterostructures. They have been attracting great attention due to their successful application in many device concepts, such as ultrafast optical modulators,[1] quantum-well infrared photodetectors (QWIPs),[2] and quantum cascade lasers.[3,4] Equally vast is their relevance for the study of fundamental physical properties, such as response nonlinearities[5] and quantum coherent effects.[6] The possibility of controlling by structural design the resonance parameters (oscillator strengths, lifetimes, carrier density) facilitates the engineering of the required properties and enables new functionalities.

Recently, the interaction of intersubband excitations with the confined electromagnetic field of a semiconductor microcavity has become the object of intense investigation.[7–11] The cavity field and the electronic transition can be viewed as two oscillators, which interact strongly when they are brought into resonance and the coupling is larger than any dephasing time or lifetime. As is well known in the case of excitons,[12–14] this results in a coherent periodic energy exchange between the excitation and the quantized electromagnetic field, with the formation of new elementary quasiparticles. The latter are eigenstates of the full photon-matter Hamiltonian, and are usually called cavity polaritons. The coupled modes exhibit an anticrossing in energy with a separation termed "vacuum-field Rabi splitting," in analogy to the atomic physics phenomenon.[15] Intersubband cavity polaritons were first observed through angle-dependent reflectance measurements in GaAs/AlGaAs multiple quantum wells using a resonator based on total internal reflection.[10] A clear mode splitting of several meV was detected up to room temperature. The phenomenon was later studied also in the photoconductive response of QWIP-like waveguide structures.[11]

Intersubband microcavities represent a particularly appealing system because their versatility allows for new features and regimes to be explored. One example of considerable interest is the possibility of realizing the situation in which the vacuum Rabi frequency is comparable to that of the photonic mode.[16] Another important aspect is the capability of manipulating the system ground state, a characteristic difficult to implement in excitonic microcavities. In this spirit, here we show how the mode coupling, and thereby the polariton dispersion, can be easily controlled electrically, to the limit where the Rabi splitting is suppressed and the polariton picture is destroyed. In the strong coupling scheme, the Rabi splitting of a collection of oscillators in a single-mode cavity is proportional to the square root of their number N. In essence, the ensemble of oscillators interacts collectively with the cavity field and behaves as a single one with oscillator strength N times larger, thereby increasing the rate at which energy is exchanged with the electromagnetic radiation.[17] For the case of intersubband transitions, the role of the oscillators is played by the quantum-well electrons. Their number can be easily altered by applying a gate voltage that progressively depletes the wells. Changing the gate voltage has thus the same effect as tuning the strength of the electromagnetic coupling.

The polarization selection rule for intersubband transitions dictates that there must be a component of the radiation electric field perpendicular to the quantum wells [transverse magnetic (TM) polarization]. It has been previously shown that a microcavity for oblique incidence can be implemented confining the radiation between a low-refractive index AlAs layer and the semiconductor-air interface through total internal reflection.[10] The surface reflection from a semiconductor-metal interface can also be used instead of the latter. When a metallic layer is deposited on the sample surface, the TM electric field has a maximum at the semiconductor-metal interface, which enhances the coupling with the intersubband transitions when the wells are close to the sample surface.[18]

[a)]Electronic mail: a.tredicucci@sns.it

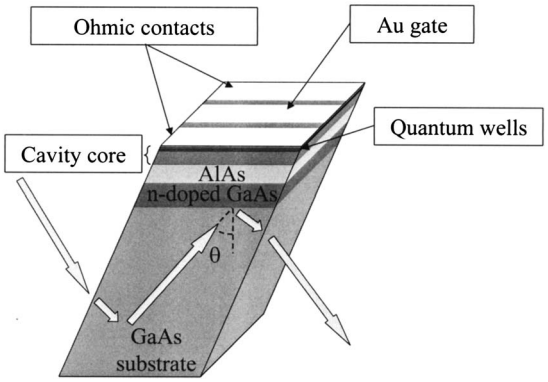

FIG. 1. Schematic view of the prism-shaped gated microcavity. The gate width was about 1.6 mm, which allowed easy focusing of the infrared light in the depleted region. The large arrows represent the optical path in the substrate.

The same metallic layer can be used as a Schottky gate to control the carrier density in the quantum wells.

Two samples were grown by solid-source molecular-beam epitaxy on an undoped GaAs (001) substrate. Their structure is schematized in Fig. 1. In both cases, the thick AlAs layer used in Ref. 10 is replaced by a 1.2 μm thick layer of GaAs n-doped to 5×10^{18} cm^{-3}, followed by a 1.5 μm thick layer of AlAs. The doped GaAs layer allowed a refractive index of 2.4, even lower than the AlAs one (at the price of some absorption). The reduced AlAs content ensured an improved structural stability of the samples. The cavity was designed for 70° angle propagation and featured three GaAs quantum wells in one sample and ten in the other. The wells were 7.5 nm thick and separated by 107 nm thick, Si-δ doped ($n_{Si}=6\times10^{11}$ cm^{-2}) $Al_{0.33}Ga_{0.67}As$ barriers. On reference samples without the doped GaAs layer, the electron density was measured to be about 5×10^{11} cm^{-2} at 1.5 K after illumination. The transition was computed to be at about 9 μm wavelength. In the three quantum well sample, a 908.5 nm thick $Al_{0.33}Ga_{0.67}As$ layer was inserted above the AlAs to give the correct cavity length. Note that due to the different boundary conditions at the metallic and total internal reflection interface, the latter was not in trivial relation with the transition wavelength. The samples were completed with a 7.5 nm GaAs cap layer to avoid Al oxidation. The gates were formed by evaporating Cr/Au with a thickness of 10/200 nm. Annealed ohmic contacts to the wells were provided by Ni/AuGe/Ni/Au with thickness 5/150/5/100 nm. The cavity reflectance was obtained by employing mechanically lapped wedge-shaped prisms, with the facets at an angle of 70° with respect to the cavity plane. The experimental procedure is detailed in a previous article.[10] In order to study the depletion of the electrons in each well, the capacitance of the sample was measured at liquid helium temperature for different gate voltages at 100 kHz with a LCR meter (HP 4284).

To investigate the coupling between the cavity mode and the intersubband transition, the cavity resonance was tuned across the intersubband one, by varying the angle of incidence. TM reflectance spectra measured at room temperature with zero gate voltage are shown in Fig. 2 for the three quantum well sample. Two dips, corresponding to the coupled cavity-intersubband modes could be clearly identified. By increasing the angle, the position of the dips shifted with a typical anticrossing behavior, manifesting the polariton dispersion. The relative Rabi splitting was observed to be about 13.2 meV at an internal angle of 68.67°. In the inset, the energy position of the dips is plotted as a function of internal angle, to better show the polariton anticrossing.

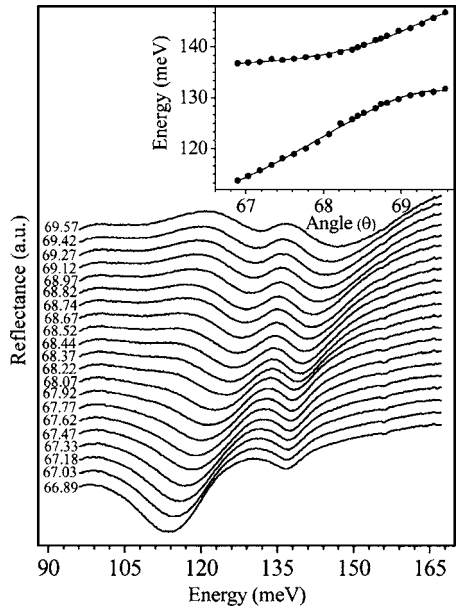

FIG. 2. Reflectance of the microcavity sample for different angles of incidence in TM polarization. The spectra were collected at 300 K, with a resolution of 2 cm^{-1}. The inset contains the experimental points corresponding to the energy position of the dips.

Figure 3 depicts the 300 K reflection spectra of the same sample at the resonance angle as a function of gate voltage. As the negative voltage applied between the gate and the quantum wells was increased, causing a progressive depletion of the wells, the magnitude of the Rabi splitting correspondingly decreased and, at about −5 V, the spectra became single-peaked signaling the transition to the so-called "weak coupling" regime and the destruction of intersubband polaritons. It is worth noting that the spectra remained symmetric around the uncoupled intersubband energy in the whole range of applied biases, with the two polariton peaks moving

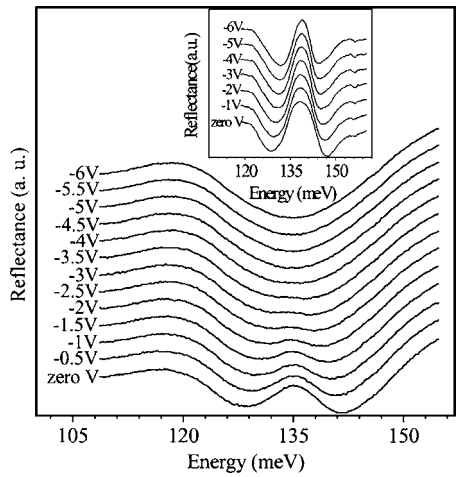

FIG. 3. Room-temperature reflection spectra of the microcavity system at the resonance angle of 68.67° as a function of gate voltage. Note that the intensity of the peak is only slightly affected by the depletion, since in this case it is mainly determined by the strength of the cavity resonance. In the inset, we report the analogous reflectance data from the ten quantum-well structure at 4 K.

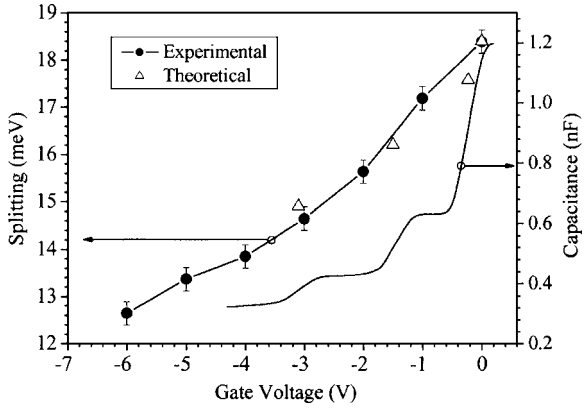

FIG. 4. The polariton splitting of the ten quantum-well structure at different gate voltages (left). Experimental data are represented by black dots and theoretical calculations by open triangles. The right line is the *C-V* curve measured between ohmic contact and gate.

in opposite directions and finally merging into a single one located in the middle. This rules out any transition shift or broadening, and clearly demonstrates the change in coupling strength induced by the electric field.

In order to understand the dependence of the normal-mode splitting on the applied voltage, we studied the ten quantum-well structures, where the sequential depletion of each well can be better followed in the evolution of the spectra. Measurements were conducted at liquid-helium temperature to lower leakage current and allow the use of capacitance-voltage $(C\text{-}V)$ curves to monitor the carrier density. The reflectance data at anticrossing are plotted in the inset of Fig. 3. The same trend as for the three quantum-well sample was observed as a function of gate voltage, with a Rabi splitting varying from 18.4 meV at zero bias to 12.7 meV at −6 V. Above −6 V, the gate became too leaky to allow for reliable determination of the electron depletion. The splitting values are plotted in Fig. 4, together with the measured device capacitance, as function of gate voltage. The *C-V* curve displayed plateaus, each corresponding to the capacitance between the gate and the uppermost occupied well. Due to surface depletion near the Schottky contact, the first well was found to be partially empty even with zero gate voltage. At a gate voltage of −3 V, the first three quantum wells were fully depleted.

The coupling between the cavity photons and the intersubband mode can be computed by modeling the structure as a multilayer stack and using the optical transfer matrix formalism. The contribution of the two-dimensional electron gas was considered by including in the dielectric constant of the quantum well layers, an additional term in the form of an ensemble of classical polarized Lorentz oscillators:

$$\varepsilon(\omega) = \varepsilon_\infty + \frac{N_s e^2 f \sin^2\theta}{m_0 \varepsilon_0 L_{\text{eff}}} \frac{1}{(\omega_0^2 - \omega^2) - i\gamma\omega}, \tag{1}$$

in which ε_∞ is the quantum-well background dielectric constant, N_s is the electronic sheet density in the well, e is the electronic charge, f is the oscillator strength of the intersubband transition, $\hbar\omega_0$ is its energy, m_0 is the electronic rest mass, ε_0 is the vacuum permittivity, γ is the intersubband linewidth, and L_{eff} is an effective quantum-well width related to the confinement of the electronic wavefunction.[10] The oscillator strength is related to the dipole matrix element d between the envelope functions of the two subbands, $f = (2m_0/\hbar)\omega_0 d^2$. In the present case, d was computed to be 1.9 nm. N_s was fixed at 5×10^{11} cm^{-2} from the reference sample. The calculated values of the Rabi splitting at the gate voltages where each quantum well was sequentially depleted (corresponding to the flex point between the plateaus) are shown in Fig. 4. We assumed that one-third of the electrons in the first well were absent, due to the surface depletion. The theoretical zero-bias value was fit to the observed one by adjusting the confinement length L_{eff} to 8.8 nm. The predicted splittings were well in line with the experimental findings.

Our results prove the mechanism for electrically controlling the polariton coupling and confirm the versatility of the system. They pave the way for the observation of novel microcavity effects and the implementation of a new concept for ultrafast electro-optic modulators.

The authors acknowledge F. Beltram, R. Köhler, V. Piazza, G. La Rocca, and C. Ciuti for their help and for useful discussions. The work was supported in part through the advanced project ICONS of INFM.

[1] S. Noda, T. Uemura, T. Yamashita, and A. Sasaki, J. Appl. Phys. **68**, 6529 (1990).
[2] H. C. Liu, in *Intersubband Transitions in Quantum Wells: Physics and Device Applications II*, Semiconductors and Semimetals, edited by H. C. Liu and F. Capasso (Academic, San Diego, 2000), Vol. 62, Chap. 2, p. 129.
[3] J. Faist, F. Capasso, D. L. Sivco, A. L. Hutchinson, and A. Y. Cho, Science **264**, 553 (1994).
[4] C. Gmachl, F. Capasso, D. L. Sivco, and A. Y. Cho, Rep. Prog. Phys. **64**, 1533 (2001).
[5] N. Owschimikow, C. Gmachl, A. Belyanin, V. Kocharovsky, D. L. Sivco, R. Colombelli, F. Capasso, and A. Y. Cho, Phys. Rev. Lett. **90**, 043902 (2003).
[6] J. Faist, F. Capasso, C. Sirtori, K. W. West, and L. N. Pfeiffer, Nature (London) **390**, 589 (1997).
[7] J. Y. Duboz, J. Appl. Phys. **80**, 5432 (1996).
[8] A. Liu, Phys. Rev. B **55**, 7101 (1997).
[9] M. Załużny, W. Zietkowski, and C. Nalewajko, Phys. Rev. B **65**, 235409 (2002).
[10] D. Dini, R. Köhler, A. Tredicucci, G. Biasiol, and L. Sorba, Phys. Rev. Lett. **90**, 116401 (2003).
[11] E. Dupont, H. C. Liu, A. J. SpringThorpe, W. Lai, and M. Extavour, Phys. Rev. B **68**, 245320 (2003).
[12] C. Weisbuch, M. Nishioka, A. Ishikawa, and Y. Arakawa, Phys. Rev. Lett. **69**, 3314 (1992).
[13] A. Tredicucci, Y. Chen, V. Pellegrini, M. Börger, L. Sorba, F. Beltram, and F. Bassani, Phys. Rev. Lett. **75**, 3906 (1995).
[14] G. Khitrova, H. M. Gibbs, F. Jahnke, M. Kira, and S. W. Koch, Rev. Mod. Phys. **71**, 1591 (1999).
[15] Y. Zhu, D. J. Gauthier, S. E. Morin, Q. Wu, H. J. Carmichael, and T. W. Mossberg, Phys. Rev. Lett. **64**, 2499 (1990).
[16] C. Ciuti, G. Bastard, and I. Carusotto, Phys. Rev. B (in press).
[17] G. S. Agarwal, Phys. Rev. Lett. **53**, 1732 (1984).
[18] M. J. Kane, M. T. Emeny, N. Apsley, C. R. Whitehouse, and D. Lee, Semicond. Sci. Technol. **3**, 722 (1988).